MOTION OF SEDIMENT PARTICLES IN A
RANKINE COMBINED VORTEX

by

Pierre Y. Julien

May 1985

Civil Engineering Department
Engineering Research Center
Colorado State University
Fort Collins, Colorado  80523

CER84-85PYJ6

MOTION OF SEDIMENT PARTICLES IN A
RANKINE COMBINED VORTEX


by


Pierre Y. Julien


May 1985

Civil Engineering Department
Engineering Research Center
Colorado State University
Fort Collins, Colorado  80523

CER84-85PYJ6

# TABLE OF CONTENTS

## ACKNOWLEDGMENTS

## LIST OF FIGURES

## LIST OF TABLES

## LIST OF SYMBOLS

$a_r$      radial acceleration of a solid particle

$a_t$      tangential acceleration of a solid particle

$a_{vr}$      radial acceleration due to viscous forces

$a_{vt}$      tangential acceleration component due to viscous forces

$C$      sediment concentration

$C_{r_o}$      sediment concentration at $r_o$

$C_\infty$      sediment concentration at infinity

$C_D$      drag coefficient

$d_s$      diameter of a solid particle

$e$      rate of energy dissipation for one particle

$E$      rate of energy dissipation per unit length

$E_{for}$      rate of energy dissipation per unit length in the forced vortex core

$E_{free}$      rate of energy dissipation per unit length in the free vortex zone

$E_k$      kinetic energy per unit length

$F_c$      centrifugal force on a solid particle

$F_p$      pressure force on a solid particle

$F_v$      viscous force on a solid particle

$L$      unit length

$n$      number of solid particles

$p$      pressure

$p_o$      pressure at the center of the vortex

$p_\infty$      pressure at $r = \infty$

$r$      radial distance from the center of the vortex

| | |
|---|---|
| $r_o$ | radius of the vortex core |
| Re' | Reynolds number using the relative velocity of the particle |
| Re | Reynolds number of the particle using the fluid velocity |
| u | tangential velocity of the fluid |
| v | total velocity of a solid particle |
| $v_r$ | radial velocity of a solid particle |
| $v_t$ | tangential velocity of a solid particle |
| v' | velocity of the particle relative to the fluid velocity |
| $v'_e$ | limit radial velocity of the particle |
| $\alpha$ | parameter governing the sediment concentration profile |
| $\Gamma$ | circulation |
| $\varepsilon$ | diffusion coefficient |
| $\nu$ | kinematic viscosity of the fluid |
| $\rho$ | mass density of the fluid |
| $\rho_s$ | mass density of the solid particles |
| $\psi$ | angle between the radial and tangential components of a particle velocity relative to the fluid |
| $\omega$ | vorticity |
| $\Omega$ | angular velocity of the forced vortex |

# I. INTRODUCTION

Turbulence is the most important factor controlling the suspension of sediments in streams. The turbulent motion of a flowing fluid results from vortex filaments formed continuously by the shearing action of the fluid. In their analysis, eddies are commonly replaced by a Rankine combined vortex which is essentially a rotational vortex core surrounded by a free vortex zone.

As opposed to flow in homogeneous fluids, the flow characteristics in a water-sediment mixture are obscured by the presence of solid particles. The motion of sediment particles in a vortex differs from the circular motion of fluid particles due to the difference in density between fluid and solid particles.

This research report presents a theoretical analysis of forces exerted on solid particles in a Rankine combined vortex. Fundamental concepts of velocity and pressure distribution in a vortex are introduced in Chapter II. The analysis of forces exerted on particles is detailed in Chapter III to define the acceleration components and the limit velocity of small particles in a vortex. The diffusion equation is introduced in Chapter IV to determine the steady-state sediment concentration profile while the rate of energy dissipation is treated in Chapter V. An experimental investigation is presented in Chapter VI.

## II.  VELOCITY AND PRESSURE DISTRIBUTION IN A RANKINE COMBINED VORTEX

Fundamental properties of the Rankine combined vortex to be used in the following theoretical analysis are presented in this chapter.  For a more complete treatment of vortex motion, the interested reader is referred to Lamb (1932), Prandtl and Tietjens (1934), Sedov (1959), Rouse and Hsu (1951), Rouse (1966), Fortier (1967), Happel and Brenner (1973) and Daily and Harleman (1973).

The mathematical concept of vorticity is known as a vector quantity $\omega$ having three orthogonal components, each of which is expressible in terms of transverse gradients of the velocity vector.  The vorticity $\omega$ is equal to twice the angular velocity $\Omega$ of a fluid element and the product of vorticity by the cross-sectional area defines the circulation $\Gamma$ which is constant along a vortex filament.  As schematized in Fig. 1 the Rankine combined vortex is composed of a forced vortex core of finite radius $r_o$ and constant vorticity $\omega$ surrounded by a free vortex of constant circulation $\Gamma = 2\pi\Omega r_o^2$.  In the following analysis, the vortex rotates around a vertical axis such that the fluid motion is in an horizontal plane.

### 2.1  Free Vortex Zone

In the free vortex zone the flow is irrotational with constant circulation.  The velocity varies inversely with the radius to satisfy the requirement of constant circulation and the boundary condition of no motion at infinity:

$$u = \frac{\Gamma}{2\pi r} \tag{1}$$

in which u is the tangential velocity at a distance r from the vortex filament.  The Bernoulli theorem for a steady irrotational flow of an inviscid incompressible fluid is:
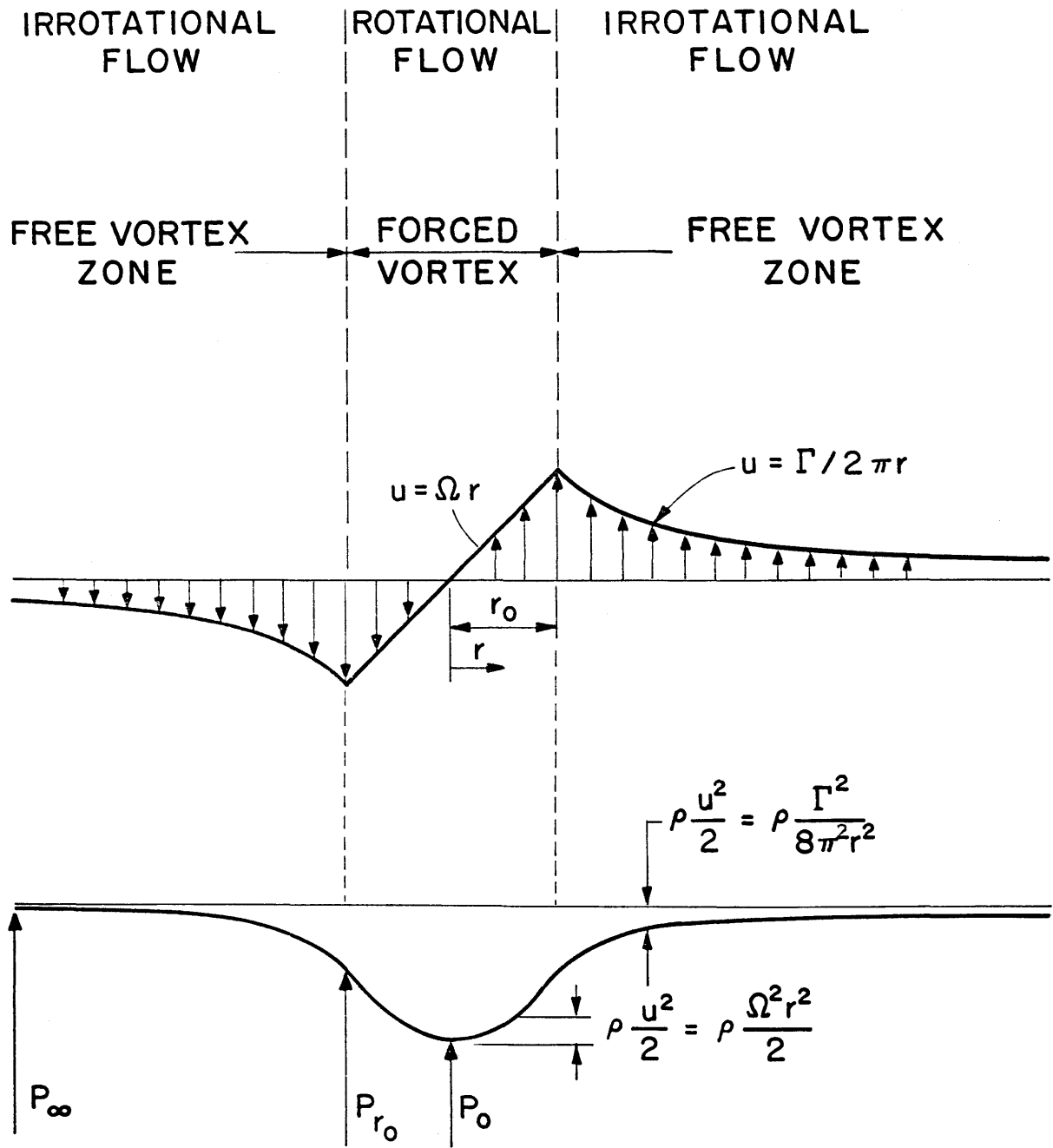
Figure 1. Velocity and pressure distribution in a
Rankine combined vortex.

$$p + \rho \frac{u^2}{2} = constant \qquad (2)$$

in which $\rho$ is the mass density of fluid; and $p$ is the pressure. The pressure distribution in a free vortex is obtained as follows from Eqs. 1 and 2 after taking the constant equal to the pressure at $r = \infty$:

$$p_\infty - p = \rho \frac{u^2}{2} = \rho \frac{\Gamma^2}{8\pi^2 r^2} \quad . \qquad (3)$$

Energy is dissipated through viscous action while the Benoulli sum along different stream lines remains constant.

## 2.2 Forced Vortex Core

In an homogeneous fluid, the forced vortex flow is rotational without any viscous energy dissipation though the Bernoulli sum between different streamlines is not constant. The velocity varies linearly with the radius ($u = \Omega r$) and the Bernoulli sum is not constant. The pressure gradient is balanced by the centrifugal acceleration:

$$\frac{1}{\rho} \frac{\partial p}{\partial r} = \frac{u^2}{r} \qquad (4)$$

and the pressure distribution is:

$$p - p_0 = \frac{\rho u^2}{2} = \frac{\rho \Omega^2 r^2}{2} \qquad (5)$$

in which $p_0$ is the pressure at the center of the vortex. Since the term $\rho u^2/2$ represents the kinetic energy per unit volume, its integral over the area of motion yields the kinetic energy $E_k$ per unit length. The total kinetic energy of the combined vortex is:

$$E_k = \rho \frac{\Gamma^2}{16\pi} + \rho \frac{\Gamma^2}{4\pi} \ln r \left.\right|_{r_0}^{\infty} \quad . \qquad (6)$$

The first term of Eq. 6 gives the kinetic energy of the forced vortex core, while the second term represents the kinetic energy of the free vortex which increases without limit in an infinite mass of fluid.

III.  FORCE EQUILIBRIUM OF A PARTICLE IN A VORTEX

The velocity and pressure distributions described in Chapter II allows us to define the forces exerted on sediment particles in a vortex.  The following analysis is focused on the motion of a small particle of diameter $d_s$ and specific mass $\rho_s$ located at distance $r$ from the center of a forced vortex. The symbol $v$ is used to describe the velocity of a particle while $u$ designates the fluid velocity.

3.1  Motion of a Particle in an Inviscid Fluid

The motion of solid particles in an inviscid fluid is investigated in this section.  The relative magnitude of pressure and centrifugal forces defines the acceleration of solid particles in a forced and a free vortex.

3.1.1  Forced Vortex

In a forced vortex the pressure gradient is balanced by the centrifugal acceleration given by Eq. 4.  The pressure force $F_p$ exerted on a small particle ($d_s$ << $r$) toward the center of the vortex is:

$$F_p = \frac{\pi}{6} \rho \, d_s^3 \, \Omega^2 \, r \ . \tag{7}$$

The magnitude of the centrifugal force $F_c$ depends on the tangential velocity of the sediment particle $v_t$ and the radius of curvature.  Assuming that the radius of curvature is equal to the distance $r$ from the center of the vortex, the centrifugal force is equal to:

$$F_c = \frac{\pi}{6} \rho_s \, d_s^3 \, \frac{v_t^2}{r} \ . \tag{8}$$

In an inviscid fluid, the radial acceleration $a_r$ of the sediment particle is given by the difference between centrifugal and pressure forces divided by the mass of the particle:

$$a_r = \frac{v_t^2}{r} - \frac{\rho}{\rho_s} \Omega^2 r \qquad (9)$$

This relationship demonstrates that fluid particles moving with the fluid ($v_t$ = u = $\Omega$r) are in equilibrium since for that case $a_r$ = 0. Another interesting situation arises when $v_t$ = 0 for which case an acceleration proportional to $\Omega^2 r$ is exerted on the particle toward the center of the vortex. When $v_t$ = u and $\rho_s > \rho$, Eq. 9 transforms to:

$$a_r = (1 - \frac{\rho}{\rho_s}) \Omega^2 r \quad ; \qquad \text{when} \quad v_t = u = \Omega r \qquad (10)$$

$$a_r = - \frac{\rho}{\rho_s} \Omega^2 r \quad ; \qquad \text{when} \quad v_t = 0 \qquad (11)$$

These equations are only valid for inviscid fluids.

### 3.1.2 Free Vortex

The motion of a particle in a free vortex can be derived using a similar procedure. The pressure gradient from Eqs. 1 and 2 is:

$$\frac{\partial p}{\partial r} = \rho \frac{\Gamma^2}{4\pi^2 r^3} \qquad . \qquad (12)$$

The pressure force exerted on the particle toward the lower values of pressure reduces to:

$$F_p = \frac{\pi}{6} \rho \frac{\Gamma^2}{4\pi^2} \left(\frac{d_s}{r}\right)^3 \qquad . \qquad (13)$$

The centrifugal force given by Eq. 8 counterbalances the pressure force and the corresponding acceleration is:

$$a_r = \frac{v_t^2}{r} - \frac{\rho}{\rho_s} \frac{\Gamma^2}{4\pi^2 r^3} \qquad . \qquad (14)$$

The radial acceleration vanishes when the velocity of buoyant particles ($\rho_s = \rho$) equals the velocity of the fluid. The particles

denser than the fluid are accelerated outward when their tangential velocity is the same as the fluid. On the other hand, a particle at rest is attracted toward the center of the vortex filament. The corresponding relationships are:

$$a_r = (1 - \frac{\rho}{\rho_s}) \frac{\Gamma^2}{4\pi^2 r^3} \quad ; \qquad \text{when} \quad vt = u = \frac{\Gamma}{2\pi r} \qquad (15)$$

$$a_r = - \frac{\rho}{\rho_s} \frac{\Gamma^2}{4\pi^2 r^3} \quad ; \qquad \text{when} \quad v_t = 0 \quad . \qquad (16)$$

These equations based on centrifugal and pressure forces exerted on particles are valid only for inviscid fluids.

## 3.2 Motion of a Particle in a Viscous Fluid

A more realistic description of the motion of a sediment particle in a vortex is given when the viscous forces are included in the analysis. The velocity components of a particle in the radial $v_r$ and tangential $v_t$ directions are assumed to differ from the fluid velocity u as shown in Fig. 2. The velocity of the particle relative to the fluid v' is equal to:

$$v' = \sqrt{v_r^2 + (v_t - u)^2} \qquad (17)$$

and the angle $\psi = \tan^{-1} v_r/v_t$ between the two relative velocity components is defined as shown in Fig. 2.

The friction force exerted on the particle is function of the relative velocity v', the Reynolds number of the particle $Re' = v'd_s/v$, the surface area and the drag coefficient $C_D$:

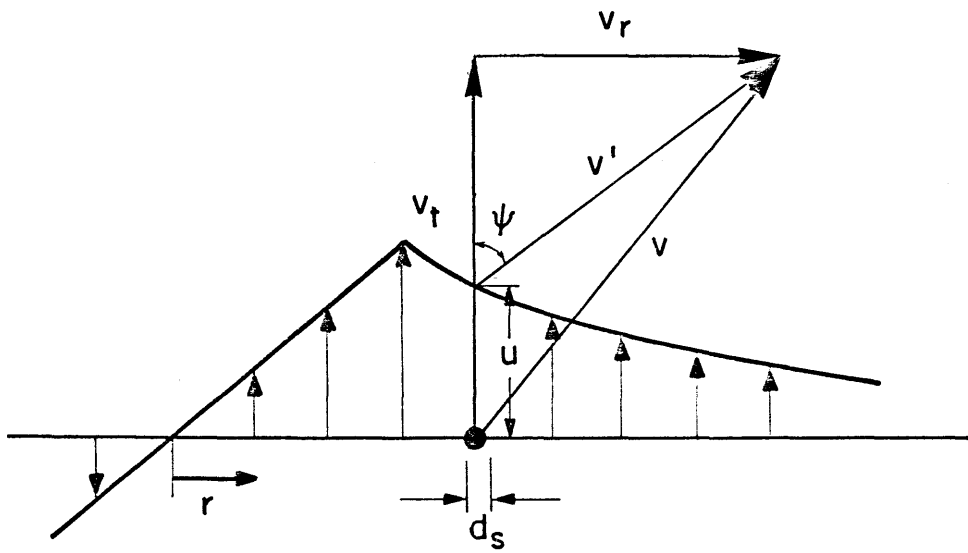$$F_V = C_D \frac{\pi d_s^2 \rho v'^2}{8} \qquad . \qquad (18)$$

Fig. 2. Relative velocity of a solid particle in a vortex.

The two components in the radial and transversal directions of the acceleration vector are:

$$a_{vr} = \frac{6 \, F_V}{\rho_s \, \pi \, d_s^3} \sin \psi \qquad , \qquad (19)$$

$$a_{vt} = \frac{6 \, F_V}{\rho_s \, \pi \, d_s^3} \cos \psi \qquad . \qquad (20)$$

The resulting force equilibrium per unit mass in the radial direction for both forced and free vortex are given from subtracting the viscous component (Eq. 19) from the previous relationships Eqs. 9 and 14 while the components in the transversal are derived from Eq. 20.

In the forced vortex zone ($r \leq r_o$):

$$a_r = \frac{v_t^2}{r} - \frac{\rho}{\rho_s} \Omega^2 r - \frac{3}{4} \frac{\rho}{\rho_s} C_D \frac{v'^2 \sin \psi}{d_s} \qquad , \qquad (21)$$

$$a_t = - \frac{3}{4} \frac{\rho}{\rho_s} C_D \frac{v'^2}{d_s} \cos \psi \qquad . \qquad (22)$$

In the free vortex zone ($r \geq r_o$):

$$a_r = \frac{v_t^2}{r} - \frac{\rho}{\rho_s} \frac{\Gamma^2}{4\pi^2 r^3} - \frac{3}{4} \frac{\rho}{\rho_s} C_D \frac{v'^2 \sin \psi}{d_s} \qquad , \qquad (23)$$

$$a_t = - \frac{3}{4} \frac{\rho}{\rho_s} C_D \frac{v'^2}{d_s} \cos \psi \qquad . \qquad (24)$$

## 3.3 Acceleration of Small Particles

When the Reynolds number of the particle ($Re' = v'd_s/\nu$) is small, the friction forces exerted on the particle are predominantly viscous and the drag coefficient $C_D$ is inversely proportional to the Reynolds number:

$$C_D = \frac{24}{Re'} = \frac{24 \, \nu}{v' d_s} \qquad . \tag{25}$$

The flow around the particle is laminar and the relative velocity of the particle $v'$ cancels out in Eqs. 21 and 23 to give the acceleration components as a function of the total velocity components only.

In the forced vortex zone $(r \le r_o)$:

$$a_r = \frac{v_t^2}{r} - \frac{\rho}{\rho_s} \Omega^2 r - 18 \frac{\rho \nu}{\rho_s} \frac{v_r}{d_s^2} \qquad , \tag{26}$$

$$a_t = - 18 \frac{\rho \nu}{\rho_s} \frac{(v_t - \Omega r)}{d_s^2} \qquad . \tag{27}$$

In the free vortex zone $(r \ge r_o)$:

$$a_r = \frac{v_t^2}{r} - \frac{\rho}{\rho_s} \frac{\Gamma^2}{4\pi^2 r^3} - 18 \frac{\rho \nu}{\rho_s} \frac{v_r}{d_s^2} \qquad , \tag{28}$$

$$a_t = - 18 \frac{\rho \nu}{\rho_s} \frac{(v_t - \Gamma/2\pi r)}{d_s^2} \qquad . \tag{29}$$

Equations 27 and 29 indicate that when the ratio $\nu/d_s^2$ is very large the tangential acceleration term becomes dominant until the velocity of the particle reaches the velocity of the fluid. Therefore, the tangential velocity of small particles should always remain close to the equilibrium condition $(v_t = u)$.

The radial acceleration in viscous fluids when $v_t = u$ simplifies Eqs. 26 and 28 to give for the forced vortex $(r \le r_o)$:

$$a_r = (1 - \frac{\rho}{\rho_s}) \Omega^2 r - 18 \frac{\rho \nu}{\rho_s} \frac{v_r}{d_s^2} \qquad ; \tag{30}$$

and for the free vortex $(r \ge r_o)$:

$$a_r = (1 - \frac{\rho}{\rho_s}) \frac{\Gamma^2}{4\pi^2 r^3} - 18 \frac{\rho\nu}{\rho_s} \frac{v_r}{d_s^2} \qquad (31)$$

## 3.4  Limit Velocity of Small Particles

Equilibrium condition in the radial direction for $v_t = u$ occurs when the acceleration component $a_r$ equals 0. The limit velocities $v'_e$ of the particles in the forced vortex is obtained from Eq. 30:

$$v'_e = \frac{1}{18} \left(\frac{\rho_s}{\rho} - 1\right) \frac{\Omega^2 r}{\nu} d_s^2 \qquad ; \qquad r \leqq r_o \qquad (32)$$

and Eq. 31 gives for the free vortex

$$v'_e = \frac{1}{18} \left(\frac{\rho_s}{\rho} - 1\right) \frac{\Gamma^2}{4\pi^2 r^3 \nu} d_s^2 \quad ; \qquad r \geqq r_o \quad . \qquad (33)$$

In both cases, the ratio $v'_e/u$ of the limit velocity to the velocity of the fluid is function of the Reynolds number of the fluid Re defined as

$$Re = \frac{u \, d_s}{\nu} \qquad ; \qquad (34)$$

$$\frac{v'_e}{u} = \left[ \frac{1}{18} \left(\frac{\rho_s}{\rho} - 1\right) \frac{d_s}{r} \, Re \right] \quad . \qquad (35)$$

From this relationship, the limit radial velocity of the particle is proportional to $\rho_s$, $d_s$ and $u$ and decreases as the viscosity $\nu$ and the radius $r$ increase.

IV.  SEDIMENT CONCENTRATION PROFILE IN A VORTEX

In a viscous fluid, sediment particles gradually reach the fluid velocity and particles heavier than the fluid are ejected outside of the vortex core.  Therefore the concentration of particles decreases toward the center, thus creating a concentration gradient across the vortex.  A diffusion process proportional to this gradient induces the transport solid particles toward the regions of lower concentration. Equilibrium conditions are reached when the flux of sediment particles due to centrifugal force is balanced by the diffusion flux in the opposite direction.  This condition can be mathematically described as follows:

$$v_e' \, C - \varepsilon \, \frac{dC}{dr} = 0 \tag{36}$$

or
$$\frac{dC}{C} = \frac{v_e'}{\varepsilon} \, dr \tag{37}$$

in which  C  is the sediment concentration by volume and  $\varepsilon$  is the diffusion coefficient.

After substituting Eq. 33 into Eq. 37, the concentration profile in the free vortex zone is described by the following integral:

$$\int \frac{dC}{C} = \frac{1}{18} \int \left( \frac{\rho_s}{\rho} - 1 \right) \frac{\Gamma^2}{4\pi^2 r^3} \frac{d_s^2}{\nu\varepsilon} \, dr \quad ; \quad r \geq r_o \quad . \tag{38}$$

With the boundary condition at infinity  $C = C_\infty$, the integration of Eq. 38 gives:

$$\ell n \, \frac{C}{C_\infty} = -\left[ \left( \frac{\rho_s}{\rho} - 1 \right) \frac{\Gamma^2}{144\pi^2 \varepsilon \nu} \frac{d_s^2}{r_o^2} \right] \frac{r_o^2}{r^2} \quad . \tag{39}$$

A parameter $\alpha$ describing the distribution of sediments is defined as follows:

$$\alpha = \left(\frac{\rho_s}{\rho} - 1\right) \frac{\Gamma^2}{144\pi^2\varepsilon\nu} \left(\frac{d_s}{r_o}\right)^2 \qquad . \tag{40}$$

After substituting $\alpha$ into Eq. 39, one obtains:

$$\frac{C}{C_\infty} = e^{-\alpha \frac{r_o^2}{r^2}} \qquad ; \qquad r > r_o \qquad . \tag{41}$$

The boundary condition at $r = r_o$ is:

$$\frac{C_{r_o}}{C_\infty} = e^{-\alpha} \qquad . \tag{42}$$

This relationship shows that when $\alpha > 0$, or $\rho_s > \rho$ the concentration at $r = r_o$ is smaller than the concentration at infinity while the converse is also true when $\rho_s < \rho$.

In the forced vortex core the concentration profiles are derived from the substitution of Eq. 32 into Eq. 37:

$$\frac{dC}{C} = \frac{1}{18} \left(\frac{\rho_s}{\rho} - 1\right) \frac{\Omega^2 d_s^2}{\nu\varepsilon} r \, dr \qquad ; \qquad r \leq r_o \qquad . \tag{43}$$

Using $\Gamma = 2\pi\Omega r_o^2$ and integrating Eq. 43 gives:

$$\ell n \, \frac{C}{C_o} = \left[\left(\frac{\rho_s}{\rho} - 1\right) \frac{\Omega^2 d_s^2}{36\nu\varepsilon} r_o^2\right] \frac{r^2}{r_o^2} = \alpha \, \frac{r^2}{r_o^2} \qquad . \tag{44}$$

With the boundary condition at $r = r_o$, Eqs. 42 and 44 are combined to yield the following two relationships for the sediment concentration in a forced vortex:

$$C_o = C_\infty \, e^{-2\alpha} \qquad ,$$

$$\frac{C}{C_\infty} = e^{\alpha \left( \frac{r^2}{r_o^2} - 2 \right)} \qquad ; \quad r \leq r_o \quad . \qquad (45)$$

The concentration profiles in a Rankine combined vortex with various $\alpha$ values are shown in Fig. 3 as a function of $r/r_o$. These relationships are valid for small particles in the laminar viscous flow regime under steady-state conditions of motion.

It is concluded from this analysis that the concentration is constant when $\alpha = 0$ which correspond to infinitely small particles or the case of neutrally buoyant particles $\rho_s = \rho$. The curves for $\alpha > 0$ indicate a decrease in concentration toward the center of the eddy while the concentration in the eddy filament increases toward the center when $\rho_s < \rho$. Interestingly the ratio $C_{r_o}/C_\infty$ is equal to the square root of $C_o/C_\infty$.

$$\alpha = \left( \frac{\rho_s}{\rho} - 1 \right) \frac{\Gamma^2}{144\pi^2 \epsilon \nu} \left( \frac{d_s}{r_0} \right)^2$$
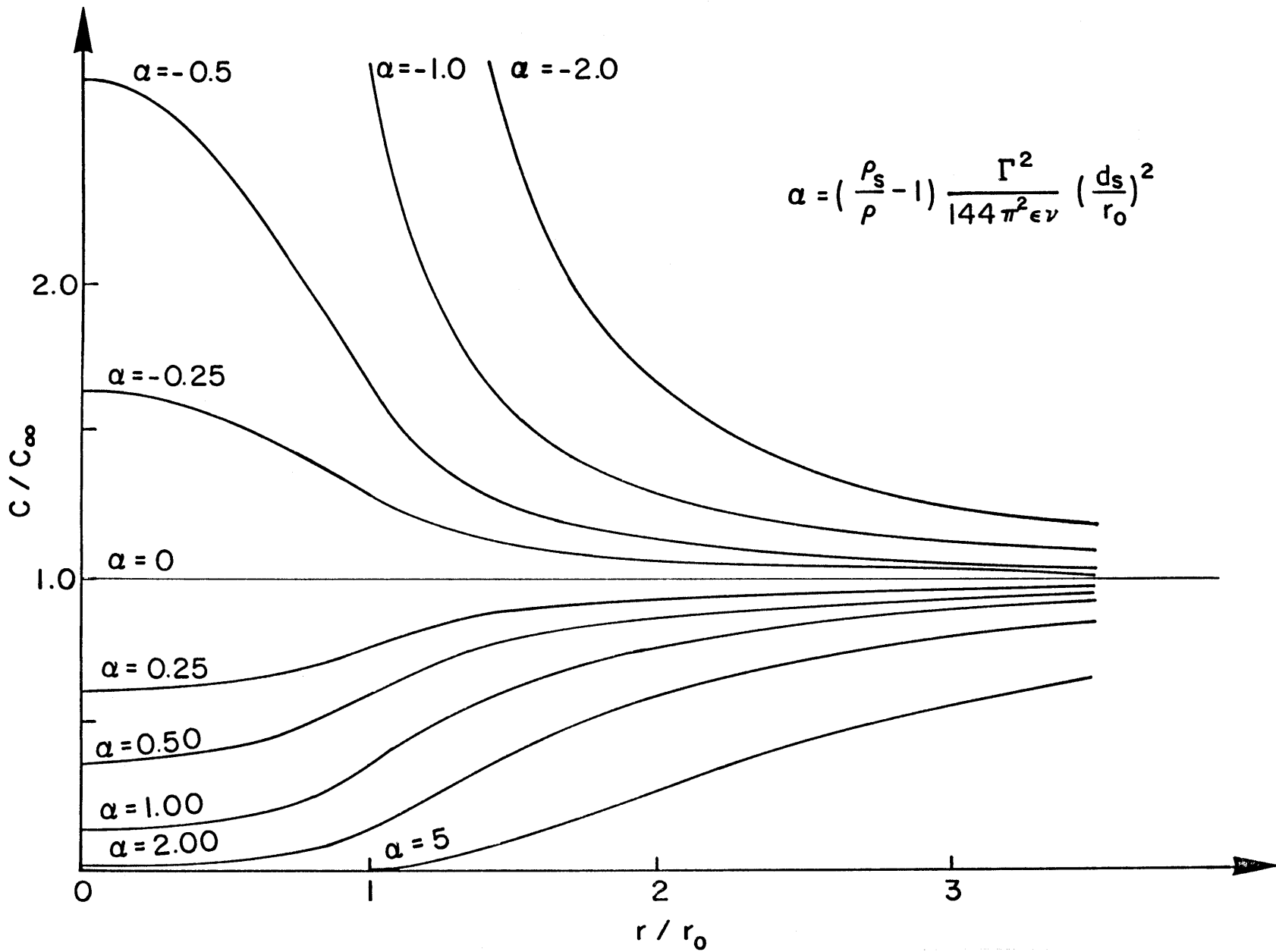
Figure 3.   Steady-state sediment concentration profile in a Rankine combined vortex.

## V.  ENERGY DISSIPATION COMPONENT DUE TO MOTION OF PARTICLES IN A VORTEX

The rate of energy expenditure  e  of one particle moving at a different velocity than the fluid is function of the density of the fluid, the kinematic viscosity  $\nu$ , the relative velocity  $v'$  and the particle size  $d_s$ . The rate of energy expenditure corresponds to the product of the friction force acting on the particle  $(3\pi\rho\nu v'd_s)$  by its relative velocity  $v'$ , as follows:

$$e = 3\pi \rho \nu v'^2 d_s \quad . \tag{46}$$

In a water-sediment mixture the number of particles per volume  $L^3$  is function of the concentration by volume  C  and the size of the particles as follows:

$$C = \frac{n \pi d_s^3}{6 L^3} \quad , \tag{47}$$

or

$$d_s = L \sqrt[3]{\frac{6C}{n\pi}} \quad . \tag{48}$$

When the concentration is uniform throughout the vortex, the rate of energy dissipation  $E = ne$  due to the motion of  n  solid particles per unit length perpendicular to the plan of vortex motion is given by:

$$E \sim \rho \nu v'^2 \sqrt[3]{n^2 C} \sim \rho \nu CL^2 \frac{v'^2}{d_s^2} \quad . \tag{49}$$

This equation simply states that the rate of energy dissipation is proportional to the viscosity, the relative velocity of the particles, the number of particles and the concentration. At a given concentration, the number of particles is function of the particle size and as was demonstrated previously, small particles tend to move at the same

velocity as the fluid. Another important remark concerns the nonuniformity of the concentration profile when $\alpha \neq 0$. In the following attempt to define the rate of energy dissipation not only the variation of concentration along the distance from the filament center is considered but the steady-state condition of motion in the vortex is included using the limit velocities of particles. The total rate of energy dissipation when the limit velocity is given by Eq. 32 or 33 with a steady-state sediment concentration (Eqs. 41 and 45) is obtained by integration along the radius $r$. The rate of energy dissipation $E$ per unit length $L^2$ is equal to the product of $e$ from Eq. 46 by the number $n$ of particles from Eq. 47 in which $L^2$ corresponds to the integral of the surface $2\pi r dr$ from 0 to infinity as follows:

$$E = \int_0^\infty 18 \, \frac{\rho \, \nu \, C \, 2\pi r}{d_s^2} \, v_e'^2 \, dr \quad . \tag{50}$$

This integral can be subdivided into two integrals since the velocity of the fluid follows different relationships for the forced and the free vortex. In the forced vortex zone, from Eqs. 45 and 32:

$$E_{for} = \int_0^{r_o} 18 \, \frac{\rho \, \nu \, 2\pi}{d_s^2} \, C_\infty \, e^{\alpha\left(\frac{r^2}{r_o^2} - 2\right)} \left[\frac{4}{3} \left(\frac{\rho_s}{\rho} - 1\right) \frac{d_s}{r} \frac{\Omega^2 r^2 d_s}{\nu}\right]^2 \, r dr \, , \tag{51}$$

$$E_{for} = 64\pi \, \frac{\rho \nu C_\infty}{d_s^2} \left[\left(\frac{\rho_s}{\rho} - 1\right) \frac{\Omega d_s^2}{\nu}\right]^2 \Omega^2 r_o^4 \int_0^1 e^{\alpha\left(\frac{r^2}{r_o^2} - 2\right)} \left(\frac{r}{r_o}\right)^3 d\left(\frac{r}{r_o}\right) \, , \tag{52}$$

$$E_{for} = 64\pi \; I_{for} \; \rho \left(\frac{\rho_s}{\rho} - 1\right)^2 \Omega^4 r_o^4 C_\infty \frac{d_s^2}{\nu} \tag{53}$$

in which
$$I_{for} = \int_0^1 e^{\alpha\left(\frac{r^2}{r_o^2} - 2\right)} \left(\frac{r}{r_o}\right)^3 d\left(\frac{r}{r_o}\right) \tag{54}$$

The integral $I_{for}$ has been evaluated for different $\alpha$ values using Simpons's rule with 20 intervals. The results of this integration are summarized in Table 1 for different values of $\alpha$. The rate of energy dissipation is proportional to $C_\infty d_s^2 / \nu$.

Table 1. Numerical integration of the rate of energy dissipation in the forced vortex core.

| $\alpha$ | $I_{for} = \int_0^1 e^{\alpha\left(\frac{r^2}{r_o^2} - 2\right)} \left(\frac{r}{r_o}\right)^3 d\left(\frac{r}{r_o}\right)$ |
|---|---|
| -10 | $2.42 \times 10^6$ |
| -5 | 422.6 |
| -2 | 4.053 |
| -1 | 0.9762 |
| -0.5 | 0.490 |
| -0.25 | 0.3495 |
| 0 | 0.250 |
| 0.25 | 0.179 |
| 0.50 | 0.129 |
| 1.0 | 0.068 |
| 2.0 | 0.019 |
| 5.0 | $0.001_6$ |
| 10.0 | $2 \times 10^{-6}$ |

The rate of energy dissipation in the core of the vortex becomes increasingly small as $\alpha$ increases since the sediment particles with $\rho_s > \rho$ are ejected outside of the core in the free vortex zone. On the

other hand, when $\alpha$ is negative, the particles lighter than the fluid dissipate more energy in the core of the vortex.

In the free vortex zone, the rate of energy dissipation is:

$$E_{free} = \int_{r_o}^{\infty} 18 \frac{\rho\nu 2\pi}{d_s^2} C_{\infty} e^{-\alpha \frac{r_o^2}{r^2}} \left[ \frac{4}{3} \left( \frac{\rho_s}{\rho} - 1 \right) \frac{\Gamma^2}{4\pi^2 r^3 \nu} d_s^2 \right]^2 r \, dr \,, \qquad (55)$$

$$E_{free} = \frac{4}{\pi^3} I_{free} \, \rho C_{\infty} \left( \frac{\rho_s}{\rho} - 1 \right)^2 \frac{\Gamma^4}{\nu} \frac{d_s^2}{r_o^4} \qquad (56)$$

in which $$I_{free} = \int_{1}^{\infty} \left( \frac{r_o}{r} \right)^5 e^{-\alpha \left( \frac{r_o}{r} \right)^2} d\left( \frac{r}{r_o} \right) . \qquad (57)$$

The integral $I_{free}$ in Eq. 57 was evaluated numerically using a Gauss-Legendre quadrature method with six points. The values of the integral are summarized in Table 2 for different values of the parameter $\alpha$. It is observed from the integral that the rate of energy dissipation vanishes as $\alpha$ becomes increasingly large.

The total energy dissipation relationship is equal to the sum of the two components in the forced vortex zone and the free vortex zone with the use of the fundamental relationship $\Gamma = 2\pi\Omega r_o^2$ the total rate of energy dissipation given from the sum of Eqs. 53 and 56 is equal to:

$$E = E_{for} + E_{free} = 64\pi (I_{for} + I_{free}) \, \rho \left( \frac{\rho_s}{\rho} - 1 \right)^2 \Omega^4 r_o^4 C_{\infty} \frac{d_s^2}{\nu} . \qquad (58)$$

the integrals $I_{for}$ and $I_{free}$ are plotted in Fig. 4 as a function of $\alpha$. This analysis shows that the rate of energy expenditure component

Table 2. Numerical integration of the rate of energy dissipation in the free vortex zone.

$$I_{free} = \int_1^\infty \left(\frac{r_o}{r}\right)^5 e^{-\alpha\left(\frac{r_o}{r}\right)^2} d\left(\frac{r}{r_o}\right)$$

| $\alpha$ | $I_{free}$ |
|---|---|
| -10 | 981.4 |
| -5 | 11.9 |
| -2 | 1.05 |
| -1 | 0.50 |
| -0.50 | 0.35 |
| -0.25 | 0.29 |
| 0 | 0.25 |
| 0.25 | 0.21 |
| 0.50 | 0.180 |
| 1.00 | 0.132 |
| 2.0 | 0.074 |
| 5.0 | 0.019 |
| 10.0 | 0.005 |

due to the motion of small particles in a Rankine combined vortex increases with sediment concentration and the particle size, and is inversely proportional to the viscosity.
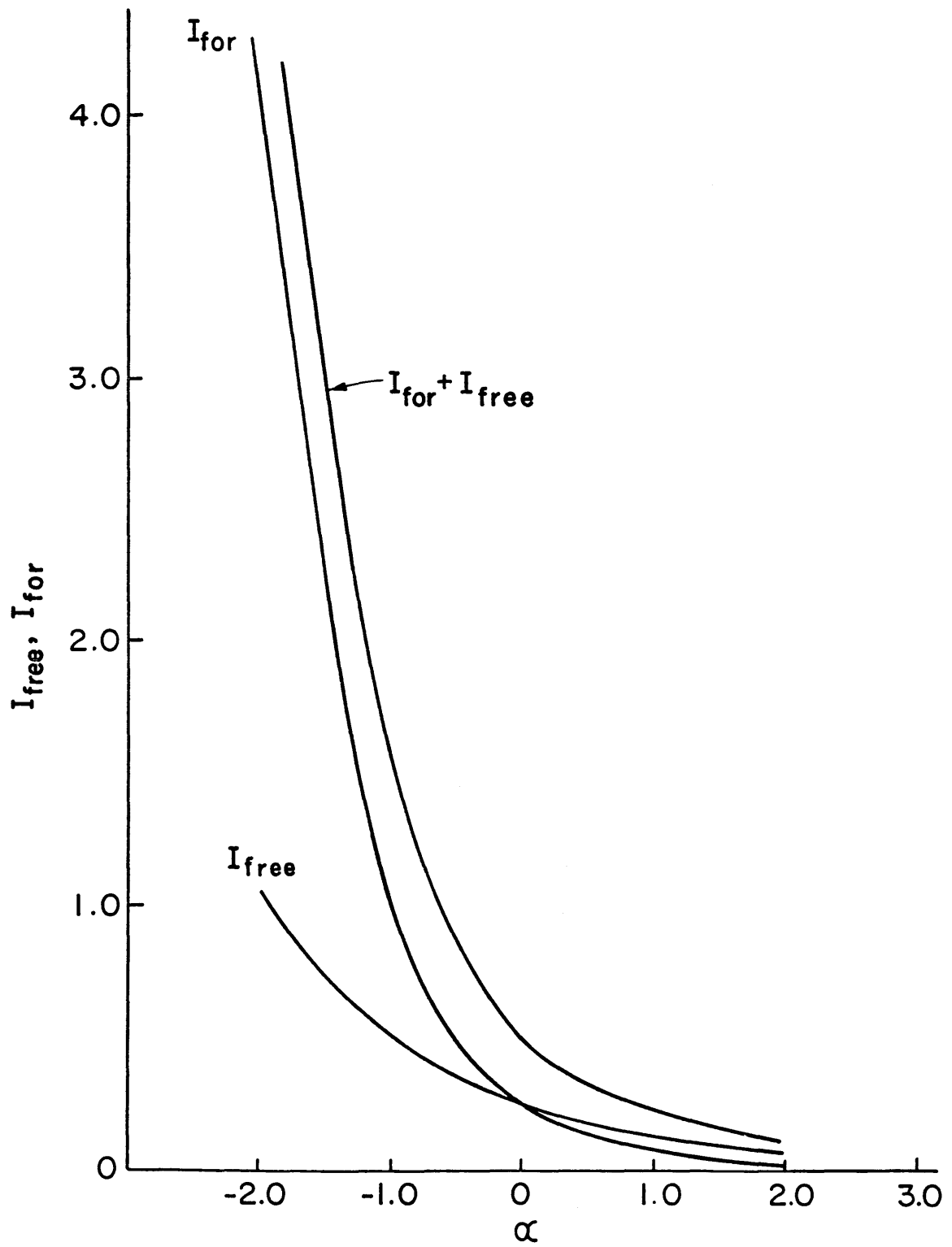
Figure 4. Values of the integrals $I_{for}$ and $I_{free}$.

## VI. EXPERIMENTAL INVESTIGATION

Laboratory experiments were conducted at the Engineering Research Center to determine the sediment concentration profile in a vortex for validation of the theoretical profiles derived in Section IV.

A water sediment mixture composed of fine sediments ($0.0053 < d_s < 0.0074$) was used for the experiments at a concentration of 50 g/L. A vortex was induced in three liters of the mixture with a 3" long magnetic stirring bar. Cross-sectional water surface profiles were measured and 30 ml samples were pipetted at several locations across the vortex to define the sediment concentration profile. The sediment concentration by weight was measured using a scale accurate to the nearest 1/10 of a milligram.

The data and their analysis are summarized in Appendix I. The circulation $\Gamma$, the angular velocity $\Omega$ and the velocity $u_o$ at the radius of the core $r_o$ are obtained from the surface profile data. The coefficients $\alpha$ and $C_\infty$ are then evaluated from the sediment concentration data after Eqs. 41 and 45 are linearized as follows:

$$\ln C = \ln C_\infty - \alpha \left(\frac{r_o}{r}\right)^2 \qquad ; \quad \text{for } r > r_o \qquad (59)$$

and

$$\ln C = \ln C_\infty + \alpha \left[\left(\frac{r}{r_o}\right)^2 - 2\right] \qquad ; \quad \text{for } r < r_o . \qquad (60)$$

In Figure 5, two sediment concentration profiles measured in this preliminary experimental study are compared with the theoretical relationships derived in Section IV (Eqs. 41 and 45). In both cases, the agreement is excellent and it is concluded that when $\rho_s > \rho$, the sediment concentration decreases toward the center of a vortex. The
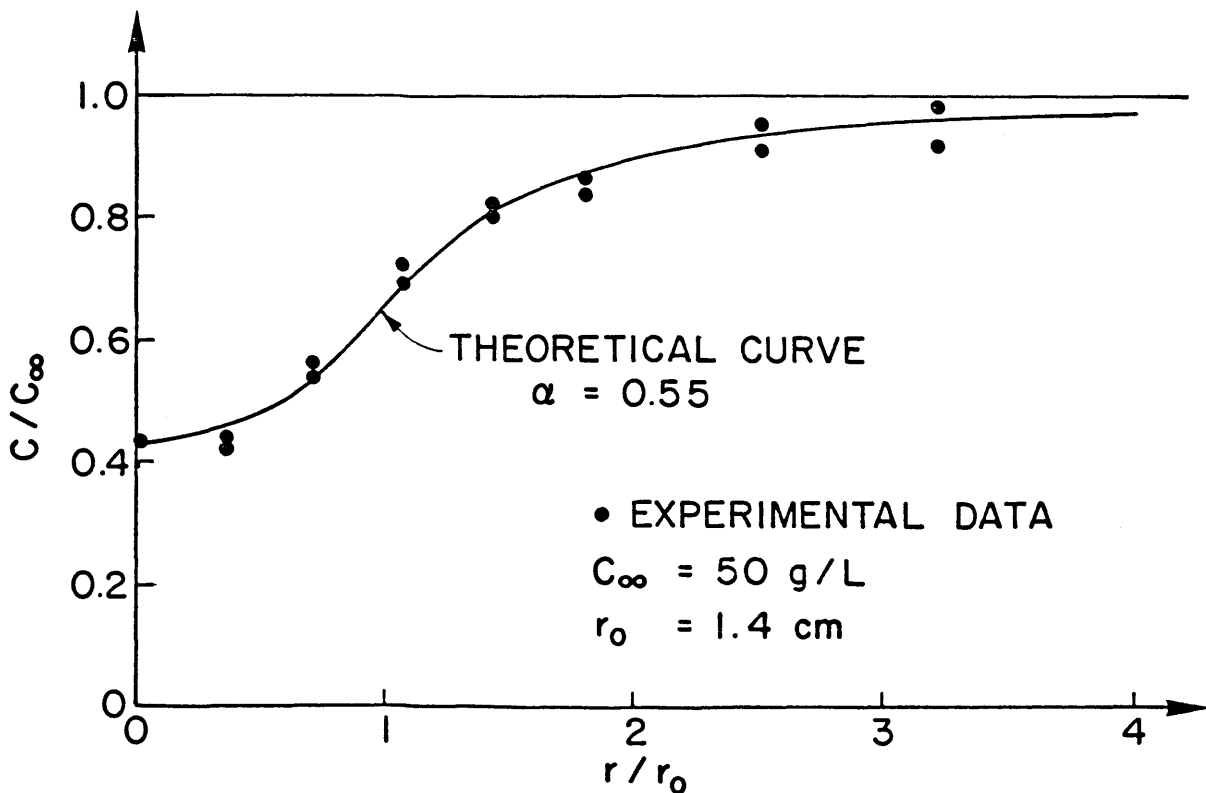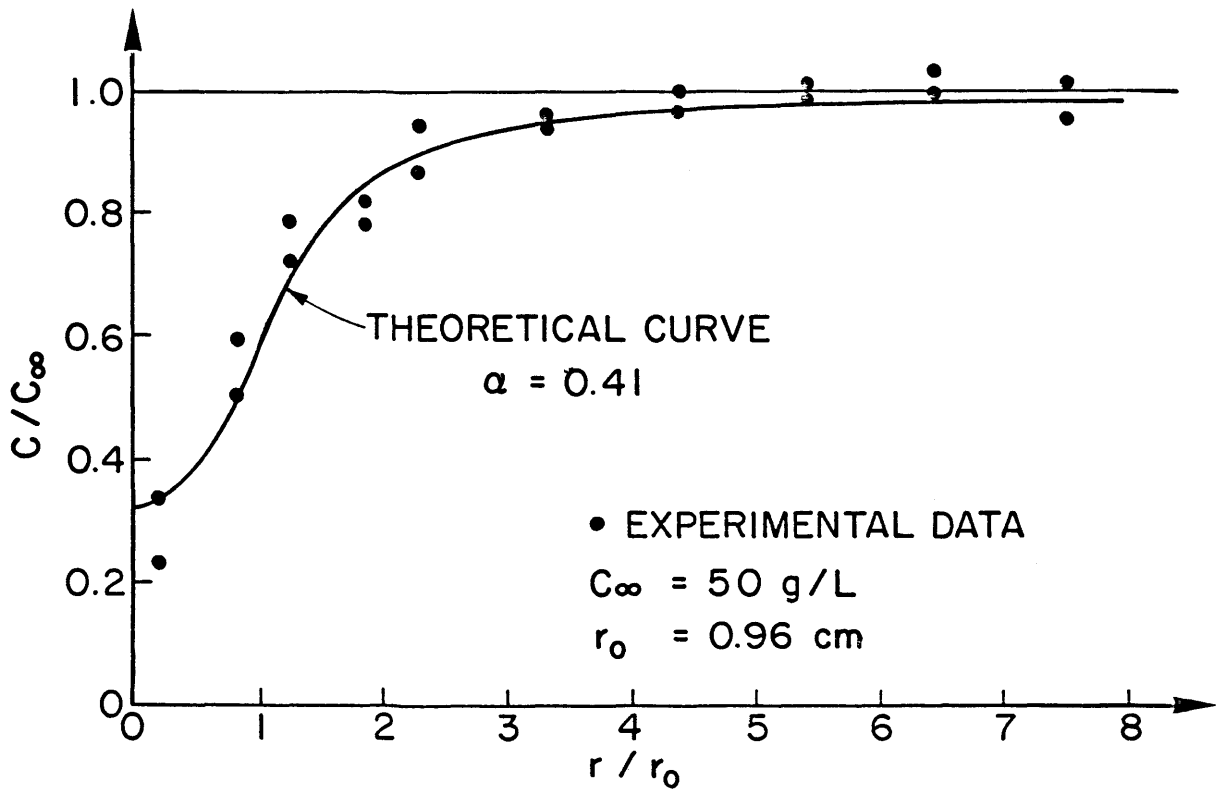
Figure 5.  Sediment concentration profiles.

sediment concentration profile as defined from Chapter IV depends on three major factors: diffusion, friction and centrifugal force on small particles.

VII. SUMMARY AND CONCLUSIONS

This report describes fundamental properties of the motion of sediment particles in a vortex. The similarities of motion for both the forced vortex and the free vortex are apparent and similar relationships for the motion of solid particles should be applicable to any vortex flow condition between pure rotational flow and pure irrotational flow.

The principal conclusions of this analysis on the force equilibrium of a particle in a Rankine combined vortex can be summarized as follows:

1) A particle at rest in the vortex is accelerated toward the center of the vortex.

2) The tangential velocity of small particles reaches rapidly the velocity of the fluid.

3) As the particles reach the tangential velocity of the fluid, the denser particles are ejected outside of the eddy and lighter particles move toward the center and the limit velocity in the radial direction is given by Eq. 35.

4) Steady-state sediment concentration profiles are defined from the limit radial velocity and the diffusion equation. The concentration profiles are shown in Fig. 3 using nondimensional scales. This theory based on pressure, centrifugal and friction forces, and diffusion is in good agreement with the measured sediment concentration profiles from this experiment (Fig. 5).

5) The relative concentration $C_{r_o}/C_\infty$ is equal to the square root of the relative concentration $C_o/C_\infty$ at the centerline of the vortex filament.

6) The rate of energy dissipation by particles moving at a different velocity than that of the fluid is proportional to the viscosity, the square of the relative velocity of the particle, the concentration of sediments and the number of sediment particles. The rate of energy dissipation at a given velocity and concentration is inversely proportional to the particle size.

## BIBLIOGRAPHY

Batchelor, G. K. An Introduction to Fluid Dynamics. Cambridge University Press, 1967, 615 p.

Daily, J. W. and D. R. Harleman. Fluid Dynamics. Addison-Wesley, 1973, 454 p.

Fortier, A. Mécanique des Suspensions, Monographie de Mécanique des Fluides et Thermique, Masson et Cie, 1967, 176 p.

Happel, J. and H. Brenner. Low Reynolds number hydrodynamics. Noordhoff International Publishing, 1973, 553 p.

Lamb, H. Hydrodynamics. Dover, 1932, 738 p.

Prandtl, L. and O. G. Tietjens. Fundamentals of Hydro and Aero-mechanics. Dover, 1934, 270 p.

Rouse, H. and H. C. Hsu. On the growth and decay of a vortex filament. Proceedings of the first national congress of applied mechanics, 1951.

Rouse, H. On the role of eddies in fluid motion, Science in Progress, Vol. 51, No. 3, Yale University Press, 1966.

Sedov, L. I. Similarity and Dimensional Methods in Mechanics. Academic Press, 1959, pp. 97-99.

APPENDIX I

ANALYSIS OF EXPERIMENTAL DATA

Two experiments A and B were conducted at the Engineering Research Center. The data collected in those experiments are presented in Tables A-1 and A-2. The pressure data $p/\gamma$ were plotted as a function of $1/r^2$ in Figure A-1 to define the circulation in the free vortex zone from the slope of the straight line fitted through the data at lower values of $1/r$:

$$\frac{p_\infty - p}{\gamma} = \frac{\Gamma^2}{8g\pi^2 r^2} \tag{A-1}$$

The radius $r_o$ is best determined from the sediment concentration profiles or from the velocity $u_o$ as follows:

$$u_o = \sqrt{g\left(\frac{p_\infty - p_o}{\gamma}\right)} \tag{A-2}$$

When Eq. A-2 is used, the radius $r_o$ and the angular velocity $\Omega$ are then defined from $u_o$ and $\Gamma$:

$$r_o = \frac{\Gamma}{2\pi u_o} \tag{A-3}$$

and $\qquad \Omega = \dfrac{u_o}{r_o}$ $\hspace{4cm}$ (A-4)

The equations for sediment concentration are linearized using the following procedure:

• In the free vortex zone, from Eq. 41,

$$\ell n\ C = \ell n\ C_\infty - \alpha\left(\frac{r_o}{r}\right)^2 \quad ; \qquad r > r_o \tag{A-5}$$

which is a linear relationship when $\ell n\ C$ is plotted as a function of $x = -\ (r_o/r)^2$. The free vortex zone is represented by $-1 < x < 0$.

Table A-1.   Data Summary - Experiment A

| Distance from Center r cm | Free Surface Elevation E cm | $W_{sed}$ g | $W_{mixture}$ g | $C_w$ g/L |
|---|---|---|---|---|
| -7.20 | 4.7 | 1.6159 | 31.5652 | 51.19 |
| -6.20 | -- | 1.5402 | 30.7621 | 50.06 |
| -5.20 | -- | 1.5432 | 31.1106 | 49.60 |
| -4.20 | -- | 1.5127 | 31.2306 | 48.43 |
| -3.20 | 4.4 | 1.4582 | 30.6222 | 47.61 |
| -2.20 | 4.2 | 1.3182 | 30.2730 | 43.54 |
| -1.20 | 3.5 | 1.2265 | 33.4187 | 36.70 |
| -0.20 | 0.0 | 0.3731 | 30.2924 | 12.31 |
| 0.80 | 2.6 | 0.9129 | 30.6786 | 29.75 |
| 1.80 | 3.3 | 1.2669 | 32.3407 | 39.17 |
| 2.80 | 4.3 | -- | -- | -- |
| 7.80 | 4.6 | -- | -- | -- |
| 1.80 | -- | 1.2486 | 30.4220 | 41.04 |
| 0.80 | -- | 0.7763 | 30.6766 | 25.31 |
| -0.20 | -- | 0.5451 | 31.7527 | 17.17 |
| -1.20 | -- | 1.1981 | 30.3124 | 39.53 |
| -2.20 | -- | 1.4284 | 30.3984 | 46.99 |
| -3.20 | -- | 1.4426 | 30.8132 | 46.82 |
| -4.20 | -- | 1.5599 | 31.2832 | 49.86 |
| -5.20 | -- | 1.6729 | 32.4291 | 51.59 |
| -6.20 | -- | 1.6557 | 31.8087 | 52.05 |
| -7.20 | -- | 1.6929 | 35.3152 | 47.94 |

Table A-2.  Data Summary - Experiment B

| Distance from Center R cm | Free Surface Elevation E cm | $W_{sed}$ g | $W_{mixture}$ g | $C_w$ g/L |
|---|---|---|---|---|
| 8.0 | 8.4 | -- | -- | -- |
| 6.5 | -- | 1.4426 | 30.5868 | 47.16 |
| 6.0 | 8.2 | -- | -- | -- |
| 5.0 | 7.8 | -- | -- | -- |
| 4.5 | -- | 1.3965 | 30.0300 | 46.50 |
| 4.0 | 7.4 | -- | -- | -- |
| 3.5 | -- | 1.3864 | 30.0149 | 46.19 |
| 3.0 | 6.4 | -- | -- | -- |
| 2.5 | 5.4 | 1.3082 | 30.7652 | 42.52 |
| 2.0 | 4.6 | 1.2880 | 31.2790 | 41.18 |
| 1.5 | 3.8 | 1.0845 | 29.9024 | 36.27 |
| 1.0 | 3.2 | 0.8505 | 29.6094 | 28.72 |
| 0.5 | 0.4 | 0.6237 | 28.1552 | 22.16 |
| 0.0 | 0.0 | 0.6169 | 28.1195 | 21.94 |
| -0.5 | 1.0 | 0.6397 | 29.1375 | 21.95 |
| -1.0 | 2.6 | 0.7869 | 28.7656 | 27.36 |
| -1.5 | 3.4 | 1.0324 | 29.6077 | 34.87 |
| -2.0 | 4.8 | 1.3002 | 31.2927 | 41.55 |
| -2.5 | -- | 1.2783 | 29.2355 | 43.72 |
| -3.0 | 6.6 | -- | -- | -- |
| -3.5 | -- | 1.4623 | 30.5686 | 47.84 |
| -4.0 | 7.4 | -- | -- | -- |
| -4.5 | -- | 1.4838 | 29.9539 | 49.54 |
| -5.0 | 8.0 | -- | -- | -- |
| -6.5 | -- | 1.5452 | 30.8910 | 50.02 |
| -7.0 | 8.4 | -- | -- | -- |
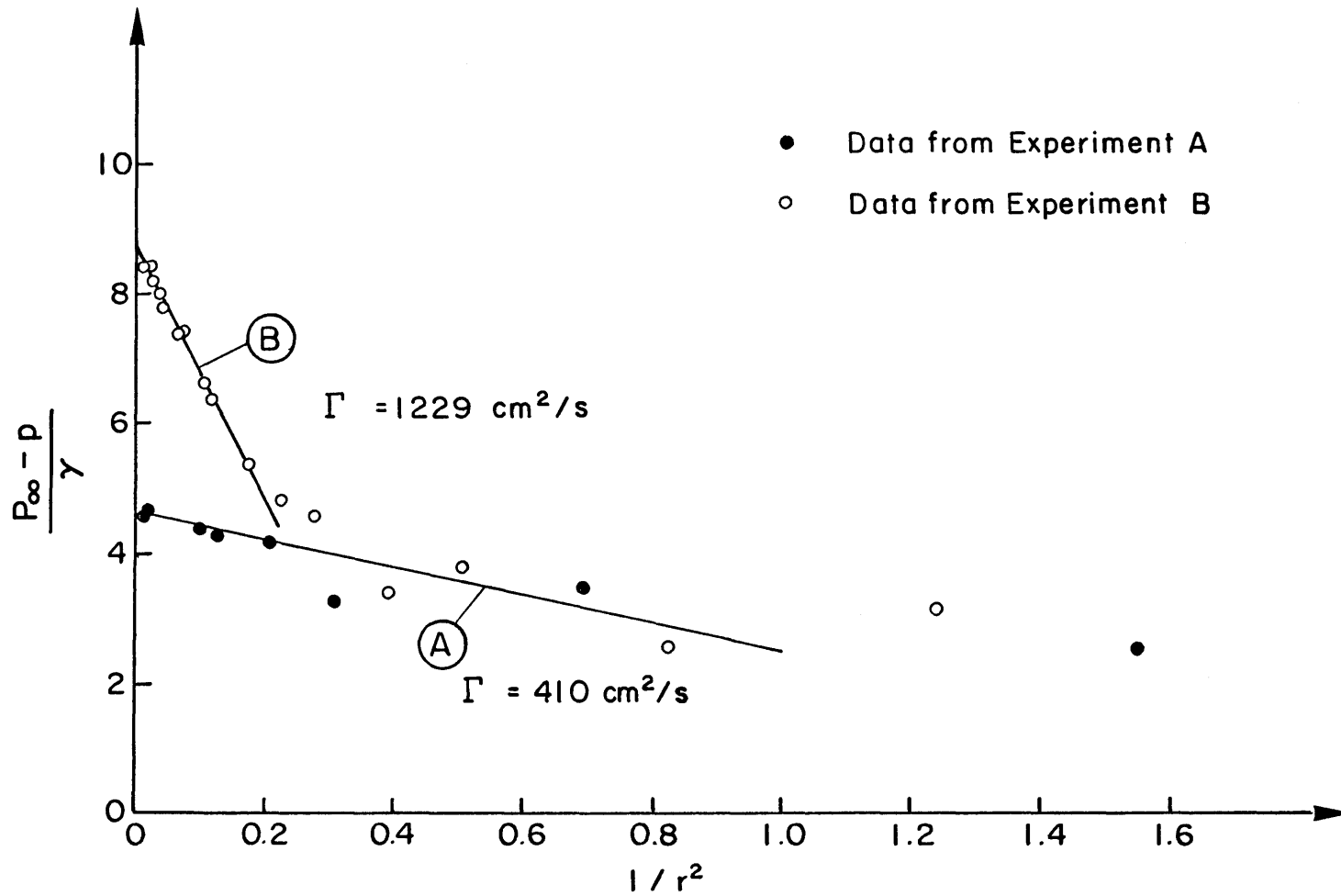
Figure A-1. Evaluation of the circulation $\Gamma$ from Experiments A and B.

- In the forced vortex core, from Eq. 45,

$$\ln C = \ln C_\infty + \alpha\left[\left(\frac{r}{r_o}\right)^2 - 2\right] \quad ; \qquad r < r_o \qquad \text{(A-6)}$$

which is a linear relationship when $\ln C$ is plotted as a function of $x = (r/r_o)^2 - 2$. The forced vortex core is represented by $-2 < x < -1$.

Examples are given in Figures A-2 and A-3 for experiments A and B. Two linear relationships are found for both the forced vortex core and the free vortex zone. It is shown in Figure A-4 for experiment B that a linear relationship valid for both zones is obtained when the appropriate value of $r_o$ is selected. For experiment B, the value $r_o = 1.4$ cm is shown to give excellent agreement with the experimental data.

The values of $\alpha$ are determined from the slope of the lines in Figures A-2 and A-4. The diffusion coefficient $\varepsilon$ is then computed from Eq. 40 when the values of $\rho_s$, $\nu$ and $d_s$ are known. For both cases A and B the parameters are summarized in Table A-3.

Table A-3. Summary of Experimental Parameters

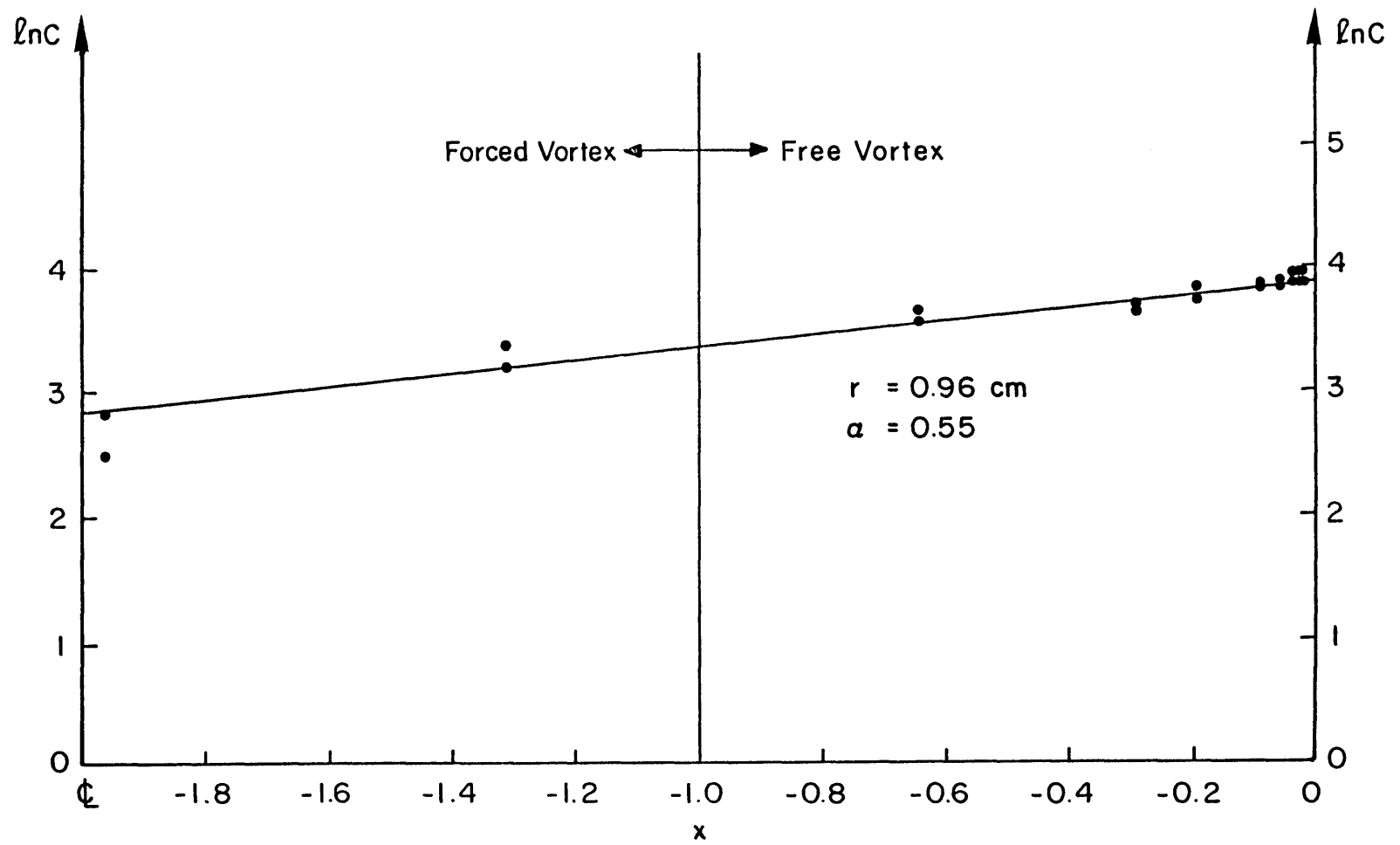| Parameters | Experiment A | Experiment B |
|---|---|---|
| $u_o$ | 68 cm/s | 140 cm/s |
| $r_o$ | 0.96 cm | 1.40 cm |
| $\Omega$ | 71/s | 100/s |
| $\Gamma$ | 410 cm$^2$/s | 1230 cm$^2$/s |
| $\alpha$ | 0.55 | 0.41 |
| $\rho_s/\rho$ | 2.73 | 2.73 |
| $d_s$ | 0.0064 mm | 0.0064 mm |
| $\nu$ | 0.01 cm$^2$/s | 0.01 cm$^2$/s |
| $\varepsilon$ | 1.67 cm$^2$/s | 9.4 cm$^2$/s |

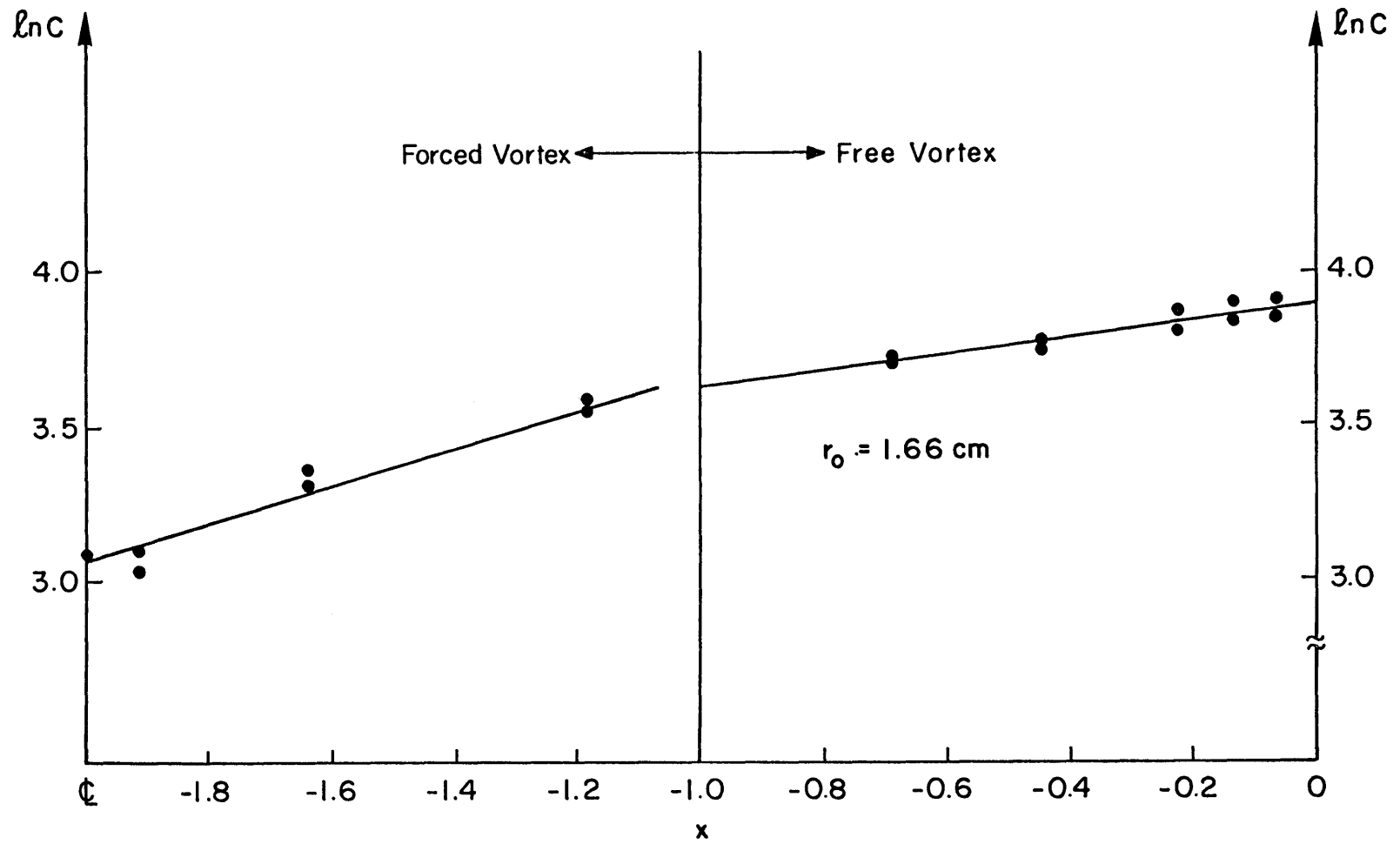Figure A-2.  Linearized sediment concentration profile - Experiment A.

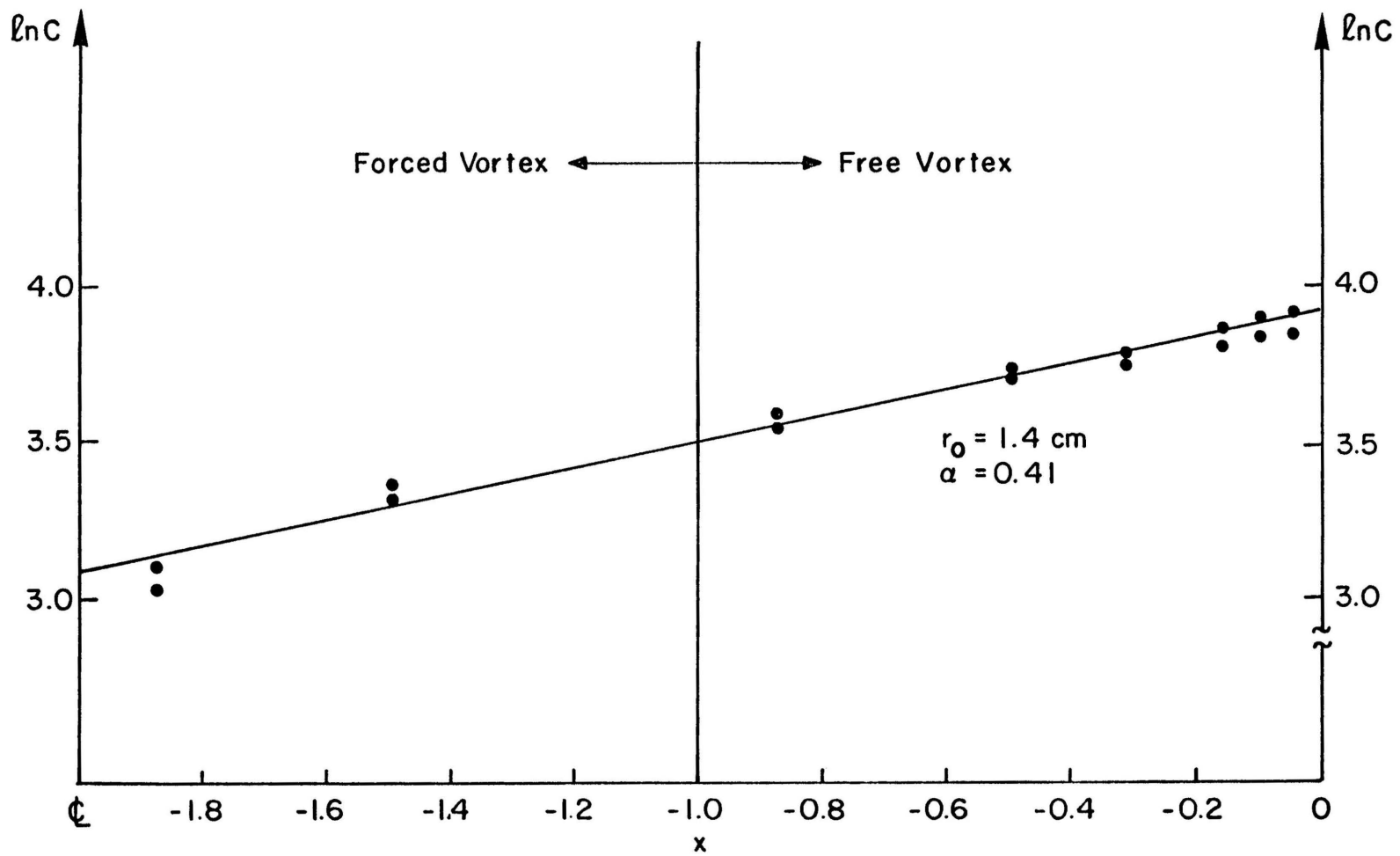Figure A-3.  Linearized sediment concentration profile - Experiment B.

Figure A-4.   Linearized sediment concentration profile - Experiment B.